nature biotechnology

Chloroplastic photorespiratory bypass increases photosynthesis and biomass production in *Arabidopsis thaliana*

Rashad Kebeish, Markus Niessen, Krishnaveni Thiruveedhi, Rafijul Bari, Heinz-Josef Hirsch, Ruben Rosenkranz, Norma Stäbler, Barbara Schönfeld, Fritz Kreuzaler & Christoph Peterhänsel

We introduced the *Escherichia coli* glycolate catabolic pathway into *Arabidopsis thaliana* chloroplasts to reduce the loss of fixed carbon and nitrogen that occurs in C_3 plants when phosphoglycolate, an inevitable by-product of photosynthesis, is recycled by photorespiration. Using step-wise nuclear transformation with five chloroplast-targeted bacterial genes encoding glycolate dehydrogenase, glyoxylate carboligase and tartronic semialdehyde reductase, we generated plants in which chloroplastic glycolate is converted directly to glycerate. This reduces, but does not eliminate, flux of photorespiratory metabolites through peroxisomes and mitochondria. Transgenic plants grew faster, produced more shoot and root biomass, and contained more soluble sugars, reflecting reduced photorespiration and enhanced photosynthesis that correlated with an increased chloroplastic CO_2 concentration in the vicinity of ribulose-1,5-bisphosphate carboxylase/oxygenase. These effects are evident after overexpression of the three subunits of glycolate dehydrogenase, but enhanced by introducing the complete bacterial glycolate catabolic pathway. Diverting chloroplastic glycolate from photorespiration may improve the productivity of crops with C_3 photosynthesis.

Many important crops are C_3 plants, in which primary CO_2 fixation is catalyzed by the enzyme ribulose-1,5-bisphosphate carboxylase/oxygenase (rubisco). Although this chloroplastic enzyme is the world's most abundant protein, it is widely regarded as being particularly inefficient owing to its capacity to catalyze both the carboxylation and oxygenation of ribulose-1,5-bisphosphate[1]. The balance between these two activities depends mainly on the CO_2/O_2 ratio in the leaves[2]. Each carboxylation reaction produces two molecules of phosphoglycerate that enter the Calvin cycle, ultimately to form starch and sucrose and to regenerate ribulose-1,5-bisphosphate. The oxygenation reaction produces single molecules of phosphoglycerate and phosphoglycolate. In C_3 plants, which include crops such as rice and wheat, the latter is recycled into phosphoglycerate by photorespiration[3,4] (**Fig. 1**). One molecule of CO_2 is released for every two molecules of phosphoglycolate produced, a net loss of fixed carbon that reduces the production of sugars and biomass. Ammonia is also lost in this reaction, and needs to be refixed through energy-consuming reactions in the chloroplast.

The negative impact of photorespiration on plant growth and yield has been demonstrated by doubling the CO_2 concentration in a glasshouse environment, dramatically increasing the performance of several crops[5,6]. However, such a strategy cannot be implemented in the field, where photorespiratory losses are also exacerbated by high temperatures and suboptimal water supplies. Under these conditions, the stomata close and the intercellular oxygen concentration increases through the release of O_2 from the light reactions of photosynthesis[7].

Despite these disadvantages, photorespiration is important because it recovers 75% of the carbon from phosphoglycolate and efficiently removes potent inhibitors of photosynthesis[8,9]. Photorespiration mutants are therefore incapable of growing at ambient CO_2 concentrations[10–12]. Moreover, photorespiration dissipates excess photochemical energy under high light intensities, thus protecting the chloroplast from over-reduction[7,13].

Many bacteria can metabolize glycolate, and *E. coli* can use glycolate as a sole carbon source[14,15] (**Fig. 1**). Like plant photorespiration, the first reaction is the oxidation of glycolate to form glyoxylate. However, the bacterial glycolate dehydrogenase (GDH) comprises three subunits and unknown organic cofactors, whereas plant glycolate oxidase is a single polypeptide that uses oxygen as a cofactor and produces peroxide. In the bacterial pathway, two molecules of glyoxylate are ligated by glyoxylate carboligase (GCL) to form one molecule of tartronic semialdehyde, and one molecule of CO_2 is released. Tartronic semialdehyde is further converted to glycerate by tartronic semialdehyde reductase (TSR). This pathway coexists and cooperates with the glycine decarboxylase pathway in the photosynthetic cyanobacterium *Synechocystis*[16].

In this study, we demonstrate reduced photorespiration in *A. thaliana* after transfer of the *E. coli* glycolate catabolic pathway to chloroplasts. This increased biomass production in the transgenic plants concomitant with improved photosynthesis.

RWTH Aachen, Institute of Biology I, Worringer Weg 1, 52056 Aachen, Germany. Correspondence should be addressed to C.P. (cp@bio1.rwth-aachen.de).

Received 19 January; accepted 13 March; published online 15 April 2007; doi:10.1038/nbt1299

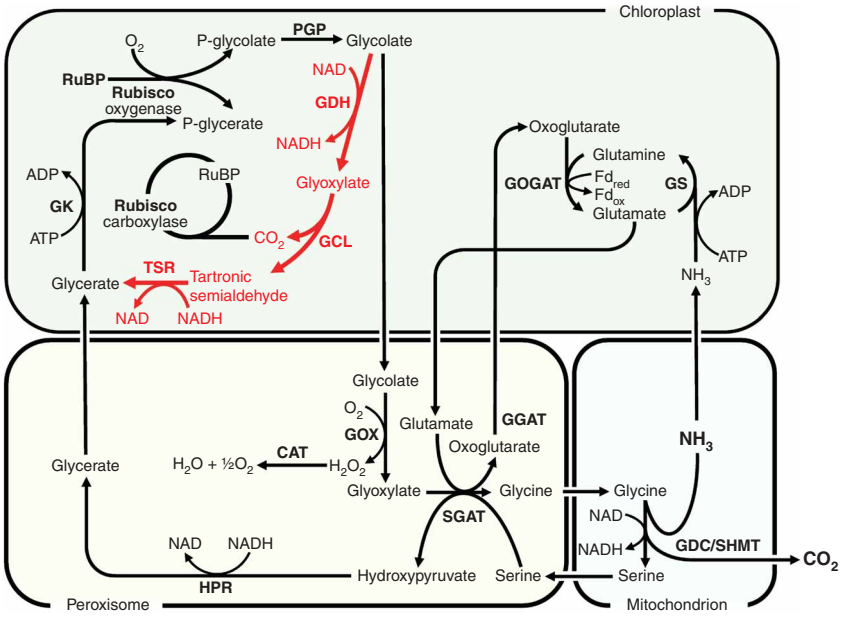

Figure 1 The *E. coli* glycolate catabolic pathway (red) superimposed on plant photorespiration (black). Rubisco, ribulose-1,5-bisphosphate carboxylase/oxygenase; RuBP, ribulose-1,5-bisphosphate; PGP, phosphoglycolate phosphatase; GOX, glycolate oxidase; CAT, catalase; GGAT, glyoxylate/glutamate aminotransferase; GDC/SHMT, glycine decarboxylase/serine hydroxymethyl transferase; SGAT, serine/glyoxylate aminotransferase; HPR, hydroxypyruvate reductase; GK, glycerate kinase; GS, glutamine synthetase; GOGAT, glutamate/oxoglutarate aminotransferase; Fd_{red}, reduced ferredoxin; Fd_{ox}, oxidized ferredoxin; GDH, glycolate dehydrogenase; GCL, glyoxylate carboxyligase; P-glycerate; phosphoglycerate; TSR, tartronic semialdehyde reductase.

RESULTS

Establishment of the pathway in *A. thaliana* chloroplasts

The *E. coli* glycolate catabolic pathway was established in *A. thaliana* chloroplasts by step-wise nuclear transformation and post-translational targeting of the proteins to plastids (for the detailed procedure, see **Supplementary Note** online). Three plasmids were used, one encoding both GDH subunits D and E, one encoding GDH subunit F and one encoding both GCL and TSR. These are referred to as constructs DE, F and GT respectively. Each plasmid also carried a different resistance marker. All genes were controlled by the constitutive cauliflower mosaic virus (CaMV) 35S promoter. Additional regulatory sequences and the targeting peptide were identical for all constructs.

For activity assays, chloroplasts were partially purified from *A. thaliana* line DEF5, which expressed all three GDH subunits. The unique properties of the plant and bacterial enzymes were exploited to distinguish the introduced activity from contaminating peroxisomal glycolate oxidase. The bacterial enzyme uses organic cofactors, is sensitive to cyanide ions and accepts D-lactate as an alternative substrate. DEF plants produced substantially more glyoxylate from glycolate compared to the wild-type plants, and this activity was inhibited by cyanide (**Fig. 2a**). Similar results were obtained in D-lactate dehydrogenase assays—DEF plants showed enhanced activity that was also sensitive to cyanide (**Fig. 2b**). This suggests that all three bacterially derived subunits are targeted to chloroplasts and assemble to form a functional GDH.

Real-time RT-PCR assays of transcript abundance were used to select plants overexpressing bacterial GCL and TSR (GT plants; data not shown) and the activities of both enzymes were tested using a coupled assay. NAD^+ generation by chloroplastic extracts from GT plants depended on the availability of glyoxylate (**Fig. 2c**). This suggests that GCL produces tartronic semialdehyde as a substrate for the TSR reaction, which in turn uses NADH as a cofactor. No substrate-dependent activity was observed in control extracts from wild-type plants. The data indicate that both GCL and TSR are active inside the chloroplast.

The full pathway was assembled by crossing GT and DEF plants. Plants containing all constructs were selected by multiplex PCR (**Supplementary Fig. 1** online) and expression levels were verified by real-time RT-PCR (data not shown). We were not able to generate lines homozygous for all constructs because transgene expression was strongly reduced in these plants, probably owing to homology-dependent gene silencing[17]. Thus, all further experiments were performed with lines that were hemizygous for some of the transgenes. Unless specified, descendants from the lines DEF5 and GT-DEF12 were selected on suitable antibiotics and used for physiological and growth assays without further evaluation of gene expression levels.

Enhanced biomass production in DEF and GT-DEF plants

Representative photographs of wild-type, DEF and GT-DEF plants are shown in **Figure 3a**. Both classes of transgenics show a substantial increase in rosette diameter. This effect is not observed in plants overexpressing incomplete glycolate dehydrogenase (DE, F) or in GT

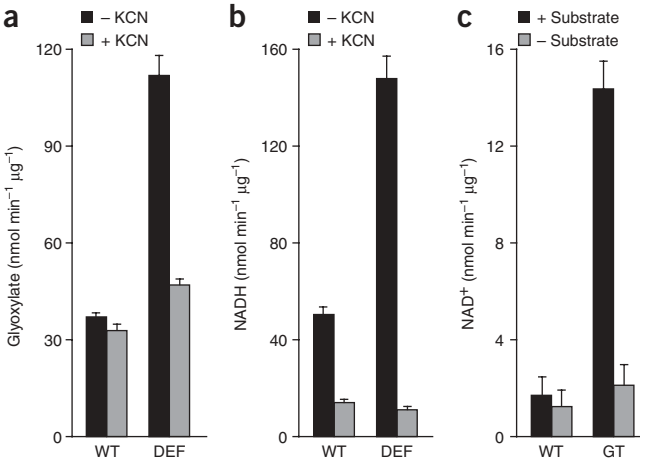

Figure 2 Activities of the bacterial enzymes in chloroplast extracts. Chloroplasts were isolated from descendants of transgenic lines and wild-type (WT) plants. Genotypes are described in the main text. (**a**) Glycolate dehydrogenase assay. (**b**) D-lactate dehydrogenase assay. (**c**) Coupled assay for glyoxylate carboligase and tartronic semialdehyde reductase. DEF, plants overexpressing subunits D, E, and F of *E. coli* glycolate dehydrogenase; GT; plants overexpressing glyoxylate carboligase and tartronic semialdehyde reductase. Controls are indicated in the figure. Each data point is based on at least three independent measurements. Error bars indicate s.e.m.

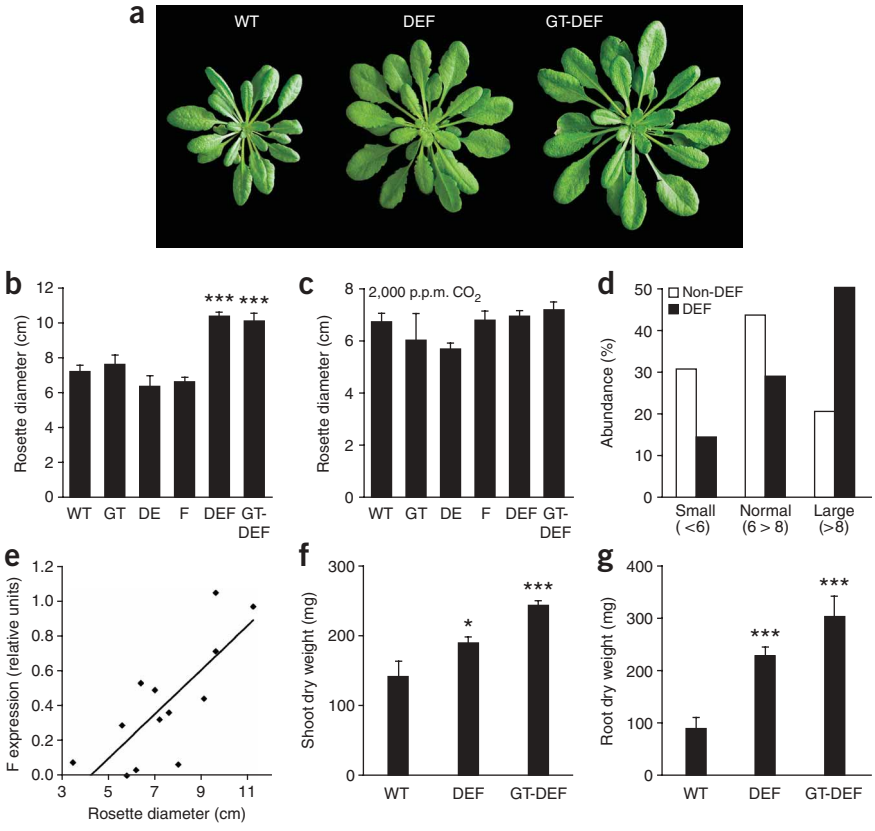

Figure 3 Growth parameters of transgenic (DEF, GT-DEF) and wild-type (WT) lines. (**a**) Representative photographs of selected transgenic plants. (**b**) Rosette diameters of plants grown at ambient conditions. (**c**) Rosette diameters of plants grown at elevated CO_2 (2,000 p.p.m.). (**d**) Abundances of small (<6 cm rosette diameter), normal (6-8 cm) and large (>8 cm) plants in a segregating population dependent on the genotype. DEF, plants containing the DE and F transgenes; non-DEF, all other genotypes. (**e**) Correlation of abundance of transcript encoding the F subunit of GDH with rosette diameter in descendants from a segregating population. (**f**) Shoot dry weights of plants grown under ambient conditions. (**g**) Root dry weights of plants grown under ambient conditions. DEF, plants overexpressing subunits D, E, and F of *E. coli* glycolate dehydrogenase; GT-DEF, plants overexpressing the complete *E. coli* glycolate catabolic pathway as shown in **Figure 1**. Each data point represents at least five independent plants. Error bars indicate s.e.m.; *, $P < 0.05$; **, $P < 0.01$; ***, $P < 0.001$ according to Student's *t*-test. Plants were selected on appropriate antibiotics for 2 weeks and then grown in soil for 6 weeks. Plants analyzed in **d** and **e** were directly grown in soil without antibiotic selection.

plants (**Fig. 3b**). In addition, the leaf blades of DEF and GT-DEF plants are flatter than those of wild-type plants and the petiole seems elongated. These phenotypic effects were reproducible over at least three generations for the two DEF lines tested (DEF5 and DEF7) and for three GT-DEF lines derived from them (**Supplementary Note**). However, when grown at elevated CO_2 concentrations, no size differences were observed among the tested genotypes (**Fig. 3c**).

We tested the correlation between rosette diameter and the presence of particular transgenes. Progenies of a hemizygous GT-DEF plant formed a segregating population containing the transgenes in different combinations. Grouping the descendants into three size classes and analyzing the individual genotypes by multiplex PCR (**Supplementary Fig. 1** online) revealed that DEF progenies were noticeably enriched among the largest plants. All other genotypes (e.g. DE plants, F plants or plants containing no transgene) showed a normal distribution among the three groups (**Fig. 3d**). To determine whether the phenotypic effect depended on transgene expression, we quantified the accumulation of the corresponding transcripts in individual DEF lines. We found a linear correlation ($R^2 = 0.76$, $P = 0.002$) between the expression of subunit F and the rosette diameter (**Fig. 3e**). No correlation between rosette diameter and the abundances of transcripts encoding subunits D and E was observed (data not shown). Transcripts encoding the D and E subunits are tenfold more abundant than those encoding the F subunit (data not shown), suggesting that the relative scarcity of the F subunit of GDH might limit the assembly of complete DEF complexes.

The dry weights of shoots and roots at the end of the vegetative period were also significantly ($P < 0.05$ and $P < 0.001$, respectively) enhanced in DEF plants compared to the wild type, but a further increase was observed in GT-DEF plants (**Figs. 3f,g**). This positive effect on biomass was also evident when plants were shifted to stress conditions such as high temperature or strong light, when photorespiration is increased (**Supplementary Fig. 2** online).

Next, we determined the contents of representative carbohydrates in leaves. GT-DEF plants showed higher contents of glucose, fructose and sucrose per unit leaf area, an increase not evident in DEF plants (**Table 1**). Similar contents of starch were observed in all genotypes.

The growth data indicate that plants overexpressing the bacterial glycolate catabolic pathway in their chloroplasts have greater biomass. This effect was obtained in part by the establishment of glycolate dehydrogenase activity.

Reduced photorespiration in DEF and GT-DEF plants

Expression of the bacterial glycolate catabolic pathway in chloroplasts should divert glycolate from photorespiration. We therefore used two different assays to quantify photorespiration. First, we determined the ratio of glycine and serine in leaves (Gly/Ser ratio)[18]. Under ambient conditions, the Gly/Ser ratio was similar for all genotypes (**Fig. 4a**), but after incubating plants at 100 p.p.m. CO_2 for 4 h, the Gly/Ser ratio increased by a factor of 10 for the wild type. This increase was much lower in the transgenic lines. GT-DEF plants showed final ratios <50% compared to wild type, and DEF plants showed intermediate values. These differences predominantly reflect the different glycine

Table 1 Contents of carbohydrates in wild-type and transgenic plants

Parameter[a]	WT	DEF	GT-DEF
Starch	1,510 (±203)	1,320 (±43)	1,522 (±114)
Glucose	188 (±16)	180 (±19)	227 (±15)
Fructose	40 (±3)	45 (±3)	66 (±3)***
Sucrose	328 (±23)	372 (±28)	403 (±17)*

[a]Given in μmol m^{-2}; *, $P < 0.05$; ***, $P < 0.001$; ±, s.e.m.

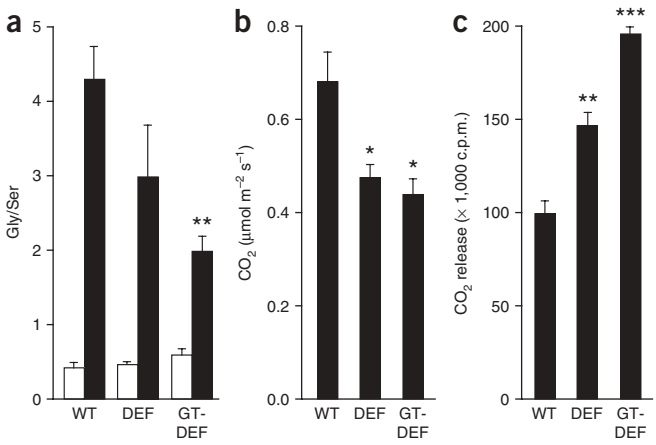

Figure 4 Reduction of the photorespiratory flow in transgenic plants (DEF, GT-DEF) compared to the wild type (WT). (**a**) Ratio of the abundances of glycine and serine in leaves of plants grown under ambient conditions (white) or shifted for 4 h to 100 p.p.m. CO_2 (black). Samples were taken 3 h after the onset of illumination. (**b**) Quantification of the postillumination CO_2 burst (PIB). (**c**) CO_2 release from glycolate in chloroplast extracts. ^{14}C-glycolate was added to chloroplast extracts and the evolving radioactive CO_2 was captured in a NaOH trap. c.p.m, counts per minute. DEF, plants overexpressing subunits D, E and F of *E. coli* glycolate dehydrogenase; GT-DEF, plants overexpressing the complete *E. coli* glycolate catabolic pathway as shown in **Figure 1**. Each data point represents at least four independent plants. Error bars indicate s.e.m.; *, $P < 0.05$; **, $P < 0.01$; ***, $P < 0.001$ according to Student's *t*-test.

contents, as the serine levels are similar in the transgenic and wild-type lines (**Supplementary Fig. 3** online).

Second, we measured the postillumination CO_2 burst (PIB) as an indicator of CO_2 release in the mitochondrial glycine decarboxylase reaction. A typical PIB profile is described in **Supplementary Fig. 4** online. DEF and GT-DEF plants showed a reduction in PIB levels of ~30% compared to the wild type (**Fig. 4b**). This confirms reduced photorespiratory flux in transgenic lines.

Enhanced CO_2 release from glycolate in chloroplast extracts

To determine the metabolic fate of glycolate, we fed labeled glycolate to chloroplast extracts from wild-type and transgenic lines. Unexpectedly, no clear spots other than the glycolate signal were observed when metabolites were separated by thin-layer chromatography (data not shown). Instead, CO_2 release from glycolate in chloroplast extracts from DEF and GT-DEF plants increased in comparison with that from the wild type (**Fig. 4c**). This suggests that the oxidation product glyoxylate is decarboxylated by GCL in GT-DEF chloroplasts. Glyoxylate decarboxylation also appears to occur in DEF plants, albeit with lower efficiency. The background activity in wild-type chloroplast extracts was not due to contamination with peroxisomal glycolate oxidase, because the peroxisomal marker enzyme catalase could not be detected in these extracts. This implies the presence of an endogenous glycolate-oxidizing enzyme in plant chloroplasts, as suggested previously[19].

Improved photosynthetic performance of DEF and GT-DEF plants

We next analyzed gas exchange and chlorophyll fluorescence parameters in wild-type and transgenic plants (**Table 2**). The apparent rate of CO_2 assimilation (A) under ambient conditions was clearly enhanced in GT-DEF plants compared to that of the wild type. DEF plants showed intermediate values. However, the maximum CO_2 fixation at saturating CO_2 concentrations was not affected. CO_2 release from glycolate in the chloroplast could be responsible for this effect and we therefore tested several parameters reflecting the CO_2/O_2 balance in the vicinity of rubisco. As anticipated, the increase in A correlated with a reduction in the oxygen inhibition of CO_2 assimilation when assimilatory rates were compared at normal (21%) and enhanced (40%) atmospheric oxygen concentrations. A similar trend was observed for the apparent CO_2 compensation point (Γ), but deviations from wild-type data were not significant. To exclude any possible indirect impact of the transgenes on CO_2 release from other metabolic pathways, for example, dark respiration in the light (R_d), we calculated the CO_2 compensation point Γ^*. For this, we determined the crossing point of several A/leaf internal CO_2 concentration curves (A/C_i) measured at different low light intensities (**Supplementary Fig. 5** online). The C_i at this point represents Γ^* and the CO_2 release by the leaf corresponds to R_d[20,21]. Also, Γ^* was significantly ($P < 0.05$) reduced in DEF plants and the effect was enhanced for GT-DEF plants with a reduction of more than 10%. However, transgene overexpression did not affect the maximum quantum efficiency of photosystem II (F_v/F_m), suggesting that differences in growth are not accounted for by differences in photoinhibition or photochemistry.

Together, these data suggest that expression of a bacterial glycolate catabolic pathway in *A. thaliana* chloroplasts enhances carbon assimilation by increasing the chloroplastic CO_2 concentration.

DISCUSSION

We established a strategy to reduce photorespiratory losses in a C_3 plant by introducing a bacterial glycolate catabolic pathway into chloroplasts. Theoretical considerations predict that the most efficient approach to reduce photorespiration may be to increase the specificity of rubisco for CO_2 through the overexpression of algal enzymes with high specificity factors[22]. Increased specificity tends to correlate with reduced catalytic rates in such enzymes[23]. Other attempts to enhance CO_2 fixation have involved introducing a C_4-like CO_2-concentrating mechanism into C_3 plants[24–26]. These strategies aim at concentrating CO_2 in the vicinity of rubisco and thus reducing the oxygenase activity of the enzyme. In our approach, the oxygenase activity is tolerated, but we divert the products of this reaction into a pathway that consumes less energy. Formally, the bacterial glycolate catabolic pathway inside the chloroplast is also a photorespiratory pathway because it involves CO_2 release and depends on O_2 fixation by rubisco.

Table 2 Chlorophyll fluorescence and gas exchange parameters of wild-type and transgenic lines

	WT	DEF	GT-DEF
A (μmol m^{-2} s^{-1}) (at C_a = 400 p.p.m)	5.5 (±0.4)	6.7 (±0.4)*	8.2 (±0.4)***
A (μmol m^{-2} s^{-1}) (at C_a = 2,000 p.p.m)	19.7 (±0.8)	19.8 (±0.6)	20.2 (±0.3)
O_2 inhibition of A (%)	36.0 (±2.9)	31.3 (±1.5)	26.2 (±0.7)*
Γ (p.p.m. CO_2)	76.3 (±2.4)	70.0 (±0.6)	67.5 (±5.4)
Γ^* (p.p.m. CO_2)	50.4 (±1.0)	46.3 (±1.2)*	44.0 (±1.5)**
R_d (μmol m^{-2} s^{-1})	0.83 (±0.06)	0.81 (±0.04)	0.79 (±0.08)
F_v/F_m	0.69 (±0.03)	0.65 (±0.04)	0.70 (±0.03)

A, apparent CO_2 assimilation; C_a, CO_2 concentration in the measuring cuvette; Γ, apparent CO_2 compensation point; Γ^*, CO_2 compensation point in the absence of dark respiration in the light; R_d, dark respiration in the light; F_v/F_m, maximum quantum efficiency of photosystem II.
*, $P < 0.05$; **, $P < 0.01$; ***, $P < 0.001$ according to Student's *t*-test; ±, s.e.m.

Even so, this technology has two major potential benefits compared to the endogenous photorespiratory pathway. First, the plastidal glycolate pathway does not release ammonia that needs to be refixed, consuming energy and reducing equivalents during conventional photorespiration[27]. Instead, the pathway produces reducing equivalents. Second, the pathway does not consume ATP, an advantage compared to C_4-like pathways where ATP is used to regenerate the CO_2 acceptor molecule. These advantages are probably most relevant under low-light conditions when energy for photosynthesis is limited. In addition, overexpression of the plastidal glycolate pathway may also improve the rescavenging of CO_2, because photorespiratory CO_2 release is shifted from the mitochondrion to the chloroplast. The PIB data indicate that there is an ~30% decrease in the abundances of precursors for the reaction catalyzed by GDH. The Gly/Ser ratio, another independent parameter that shows a linear correlation with the photorespiratory rate[18], is reduced to a similar extent. Moreover, plastidal extracts of transgenic lines release significantly ($P < 0.001$) more CO_2 from glycolate compared to those of the wild type. Such CO_2 release might improve carbon assimilation by reducing the relative oxygenase activity and by saturating the CO_2 binding site of rubisco[28]. The positive effects of CO_2 release in the chloroplasts of C_3 plants have been questioned, because this organelle has a low resistance to CO_2 diffusion[29]. Our gas exchange measurements provide several independent arguments suggesting that plastidal CO_2 concentration can be enhanced to a certain extent. First, the PIB is reduced in transgenic lines, which would not be expected when photorespiratory CO_2 release is simply shifted from one organelle to the other. Second, the oxygen inhibition of photosynthesis, a parameter that shows a strong negative correlation with the CO_2/O_2 ratio in the vicinity of rubisco[30], decreased in GT-DEF plants. Third, the CO_2 compensation point Γ^*, which provides an independent measure for the CO_2/O_2 ratio in the chloroplast, indicates that augmentation of CO_2 concentration in the chloroplast is possible.

Increased CO_2 availability is not necessarily translated directly into enhanced growth. A meta-analysis of the empirical relation between plant growth and leaf photosynthesis under laboratory conditions revealed a good correlation between these parameters[31]. Recent data from free-air CO_2 enrichment studies indicate that crop yields increase at higher CO_2 concentrations, albeit less than expected[32]. This limitation is probably due to the complex regulation of photosynthesis by, among others, the availability of nutrients[33], the negative feedback regulation of photosynthetic products on the expression and activity of photosynthetic enzymes[28,33], and the regenerative capacity of the Calvin cycle[34,35]. Such restrictions might also apply in GT-DEF plants as exemplified by the increased contents of soluble sugars, but protein gel analysis did not reveal any differences in rubisco protein content (data not shown).

The greater root and shoot biomass of GT-DEF plants indicates that they overcome at least one growth-limiting bottleneck. This effect might even be enhanced by higher expression levels of the transgenes, because transgene expression shows a positive linear correlation with biomass production and no saturation of this correlation curve was observed thus far. DEF plants performed similarly to GT-DEF plants in this experiment, but they showed effects intermediate between those of the wild-type and GT-DEF plants in most other growth and physiological assays.

There is no obvious scenario for the further conversion of glyoxylate in the chloroplast of DEF plants. Although glyoxylate could be reconverted to glycolate by the plastidal glyoxylate reductase[9,36], no net advantage would be expected from such a futile cycle. Alternatively, glyoxylate could undergo a nonenzymatic oxidative decarboxylation to formate in the presence of peroxides. Chloroplast extracts can decarboxylate externally supplied glyoxylate in the light[37–39]. A similar pathway has been proposed as part of photorespiration in some algae[40]. The formate produced could be decarboxylated further to CO_2 and H_2O by chloroplastic formate dehydrogenase[41]. As substantial GDH activity was detected in the chloroplasts of spinach[19], a related pathway may exist in wild-type plants. Overexpression of the bacterial GDH would boost this pathway and divert more glycolate from photorespiration. Admittedly, no ribulose-1,5-bisphosphate would be regenerated in any such scenario and refixation of CO_2 released from the proposed pathway would therefore be limited rapidly. Further studies are needed to elucidate precisely how glycolate oxidation in the chloroplast improves biomass production and whether such effects will also be stable under the variable growth conditions of field-grown crops.

METHODS

Plasmid constructs. The coding sequences for glyoxylate carboligase (GCL), tartronic semialdehyde reductase (TSR), *glc*D, *glc*E and *glc*F were amplified by PCR from *E. coli* DNA using suitable oligonucleotides. All sequences are available from the *E.* coli K12 genome sequence (gi49175990). GCL and TSR were cloned into the binary plant expression vector pTRAK, a derivative of pPAM (gi13508478). The expression cassettes were flanked by the scaffold attachment region of the tobacco *RB7* gene (gi3522871). The *npt*II cassette of pPCV002 (ref. 42) was used for selection of transgenic plants on kanamycin. Transcription was controlled by the enhanced CaMV 35S promoter[43] and all transgenes were translationally fused to the chloroplast targeting peptide of the potato *rbcS1* gene (gi21562). For the expression of *glc*D and *glc*E, the same vector construct was used, carrying the sulfadiazine-resistance cassette from pGABI1 (gi44894182). For the expression of *glc*F, the same vector construct was used, carrying the phosphinothricin-resistance cassette from pAM-PAT (gi38231644).

Plant growth and transformation. Stable transformation of *A. thaliana* plants ecotype Columbia (Col-0) with the respective constructs was carried out by *Agrobacterium tumefaciens* (GV3101)-mediated floral dip transformation[44]. The transgene integration sites were mapped by genome walking and are listed in **Supplementary Table 1** online. Plants used for physiological experiments were grown under short-day conditions (8 h illumination and 16 h darkness) in growth chambers at 22 °C with a photon flux density of 100 µmol m^{-2} s^{-1}. For low and high CO_2 treatments, the plants were shifted to a growth cabinet that was constantly supplied with air containing either 100 p.p.m. or 2,000 p.p.m. CO_2.

Chloroplast isolation and enzymatic assays. Intact chloroplasts were isolated from 4-week-old *A. thaliana* plants as described[45]. Approximately 5 g leaf material was ground in 50 ml grinding buffer (50 mM HEPES-KOH pH 7.5, 1 mM $MgCl_2$, 1 mM EDTA, 1 g l^{-1} BSA, 0.2 g l^{-1} sodium ascorbate, 0.3 M mannitol, 5 g l^{-1} polyvinylpyrrolidone). After filtration through three layers of Miracloth, the solution was centrifuged at 1,000*g* for 10 min. The pellets were resuspended in 1 ml SH-buffer (50 mM HEPES-KOH pH 7.5, 0.33 M sorbitol), and 0.5 ml of this solution was loaded on a 1-ml 35% Percoll gradient (35% Percoll, 65% SH-buffer). The gradient was centrifuged for 5 min at 500*g*. The chloroplast pellet was washed in 1 ml SH-buffer and chloroplast protein was extracted in 500 µl extraction buffer (50 mM HEPES-NaOH pH 7.5, 2 mM EDTA, 5 mM $MgCl_2$, 0.1% Triton X-100, 20% glycerol). Glycolate dehydrogenase and D-lactate dehydrogenase activities were measured as described[14,46]. Glyoxylate carboligase and tartronic semialdehyde reductase were assayed in a coupled reaction[47]. For labeling experiments (**Fig. 4c**), chloroplasts were loaded on an 8-ml gradient and centrifuged for 20 min at 40,000*g*. These preparations were free of contaminating catalase and fumarase activities (>95% purity).

CO_2 release from labeled glycolate in chloroplast extracts. We added 1 µCi of [1,2-^{14}C]-glycolate (Hartmann Analytics) to 50 µg of chloroplast protein extract in a tightly closed 15-ml reaction tube. Released CO_2 was absorbed in a 500-µl reaction tube containing 0.5 M NaOH attached to the inner wall of the

15-ml tube. Samples were incubated for 5 h and the gas phase in the reaction tube was frequently mixed with a syringe.

Determination of metabolites and chlorophyll contents. Two plant leaf discs (1.5 cm^2 each) were harvested after 4 h of illumination and immediately frozen. Soluble sugars were then extracted using 80% (vol/vol) boiling ethanol. Starch was extracted from bleached leaf discs and was hydrolyzed enzymatically. The glucose released from starch and the contents of soluble sugars in the ethanolic extracts were determined enzymatically[48]. For the determination of glycine and serine, whole leaf rosettes were harvested and immediately frozen in liquid nitrogen. The abundance of the amino acids was analyzed and quantified by gas chromatography/mass spectrometry using a Chemstation 5890 Series II gas chromatograph (Hewlett Packard). Extraction and derivatization of samples were performed as described[49]. A dilution series of standard substances for peak identification was prepared and a SIM-mode was implemented for quantification of each substance. The *m/z* values were: glycine (147, 174, 248), serine (116, 204, 218), ribitol (205, 217, 319). Peak areas were integrated by the auto-integration software supplied by the manufacturer.

Gas exchange and chlorophyll fluorescence measurements. Gas exchange and chlorophyll fluorescence measurements were performed using the LI-6400 system (Li-Cor) and parameters were calculated with the software supplied by the manufacturer. Conditions were: photon flux density = 1,000 μmol m^{-2} s^{-1}, chamber temperature = 26 °C, flow rate = 100 μmol s^{-1}, relative humidity = 60–70%. The oxygen inhibition of carbon assimilation (A) was calculated from A at C_a = 400 p.p.m. and atmospheric oxygen concentrations of 21% and 40%, respectively, using the equation: ox-inh.(%) = $(A_{21}\text{-}A_{40})/A_{21}$*100. The apparent CO_2 compensation point (Γ) was deduced from A/C_i curves by regression analysis in the linear range of the curve. The CO_2 compensation point in the absence of dark respiration in the light (Γ*) was measured as described[21]. The postillumination CO_2 burst (PIB) was measured under photorespiratory conditions (PFD = 1,000 μmol m^{-2} s^{-1}; C_a = 100 p.p.m.) as described[20]. The determination of Γ* and PIB is also described in **Supplementary Figures 4** and **5**.

Statistical analysis. Significance was determined according to Student's *t*-test using Excel software (Microsoft). Two-sided tests were performed for homoscedastic matrices.

Note: Supplementary information is available on the Nature Biotechnology website.

ACKNOWLEDGMENTS

This work was supported by a PhD scholarship from the Egyptian government to R.K. and grants from the Deutsche Forschungsgemeinschaft and Bayer CropScience to C.P. Thanks to Martin Parry, Alf Keys, Rainer Häusler, Veronica Maurino, Susanne von Caemmerer, John Evans, Margrit Frentzen, Dagmar Weier, Thomas Rademacher, Burkhard Schmidt and Nikolaus Schlaich for helpful discussion of this work and technical support.

AUTHOR CONTRIBUTIONS

R.K. established the transgenic lines. R.K. and M.N. conducted most of the physiological experiments. K.T. contributed to physiological and growth measurements. R.B. cloned the genes and established initial transgenic lines. H.-J.H. helped to establish enzymatic assays and metabolite measurements. R.R. established techniques for the estimation of photorespiration. N.S. and B.S. determined the chromosomal T-DNA integration sites. C.P. and F.K. designed the approach. C.P. supervised the work and wrote the manuscript.

COMPETING INTERESTS STATEMENT

The authors declare no competing financial interests.

Published online at http://www.nature.com/naturebiotechnology
Reprints and permissions information is available online at http://npg.nature.com/reprintsandpermissions

1. Mann, C.C. Genetic engineers aim to soup up crop photosynthesis. *Science* **283**, 314–316 (1999).
2. Laing, W.A., Ogren, W.L. & Hageman, R.H. Regulation of soybean net photosynthetic CO_2 fixation by the interaction of CO_2, O_2, and ribulose 1,5-diphosphate carboxylase. *Plant Physiol.* **54**, 678–685 (1974).
3. Leegood, R.C., Lea, P.J., Adcock, M.D. & Häusler, R.E. The regulation and control of photorespiration. *J. Exp. Bot.* **46**, 1397–1414 (1995).
4. Tolbert, N.E. The C2 oxidative photosynthetic carbon cycle. *Annu. Rev. Plant Physiol. Plant Mol. Biol.* **48**, 1–25 (1997).
5. Arp, W.J., Van Mierlo, J.E.M., Berendse, F. & Snijders, W. Interactions between elevated CO_2 concentration, nitrogen and water: Effects on growth and water use of six perennial plant species. *Plant Cell Environ.* **21**, 1–11 (1998).
6. Kimball, B.A. Carbon dioxide and agricultural yield: an assemblage and analysis of 430 prior obeservations. *Agron. J.* **75**, 779–788 (1983).
7. Wingler, A., Lea, P.J., Quick, W.P. & Leegood, R.C. Photorespiration: metabolic pathways and their role in stress protection. *Phil. Trans. R. Soc. Lond. B* **355**, 1517–1529 (2000).
8. Campbell, W.J. & Ogren, W.L. Glyoxylate inhibition of ribulosebisphosphate carboxylase-oxygenase: Activation in intact, lysed and reconstituted chloroplasts. *Photosynth. Res.* **23**, 257–268 (1990).
9. Givan, C.V. & Kleczkowski, L.A. The enzymic reduction of glyoxylate and hydroxypyruvate in leaves of higher plants. *Plant Physiol.* **100**, 552–556 (1992).
10. Medrano, H. *et al.* Improving plant production by selection for survival at low CO_2 concentrations. *J. Exp. Bot.* **46**, 1389–1396 (1995).
11. Somerville, C.R. The analysis of photosynthetic carbon dioxide fixation and photorespiration by mutant selection. *Oxford Surveys Plant Mol. Cell Biol.* **1**, 103–131 (1984).
12. Somerville, C.R. & Ogren, W.L. Genetic modification of photorespiration. *Trends Biochem. Sci.* **7**, 171–174 (1982).
13. Kozaki, A. & Takeba, G. Photorespiration protects C3 plants from photooxidation. *Nature* **384**, 557–560 (1996).
14. Lord, J.M. Glycolate oxidoreductase in *Escherichia coli*. *Biochim. Biophys. Acta* **267**, 227–237 (1972).
15. Pellicer, M.T., Badia, J., Aguilar, J. & Baldoma, L. glc locus of *Escherichia coli*: characterization of genes encoding the subunits of glycolate oxidase and the glc regulator protein. *J. Bacteriol.* **178**, 2051–2059 (1996).
16. Eisenhut, M. *et al.* The plant-like C2 glycolate cycle and the bacterial-like glycerate pathway cooperate in phosphoglycolate metabolism in cyanobacteria. *Plant Physiol.* **142**, 333–342 (2006).
17. Lechtenberg, B., Schubert, D., Forsbach, A., Gils, M. & Schmidt, R. Neither inverted repeat T-DNA configurations nor arrangements of tandemly repeated transgenes are sufficient to trigger transgene silencing. *Plant J.* **34**, 507–517 (2003).
18. Novitskaya, L., Trevanion, S.J., Driscoll, S., Foyer, C.H. & Noctor, G. How does photorespiration modulate leaf amino acid contents? A dual approach through modelling and metabolite analysis. *Plant Cell Environ.* **25**, 821–835 (2002).
19. Goyal, A. & Tolbert, N.E. Association of glycolate oxidation with photosynthetic electron transport in plant and algal chloroplasts. *Proc. Natl. Acad. Sci. USA* **93**, 3319–3324 (1996).
20. Atkin, O.K., Evans, J.R. & Siebke, K. Relationship between the inhibition of leaf respiration by light and enhancement of leaf dark respiration following light treatment. *Aust. J. Plant Physiol.* **25**, 437–443 (1998).
21. Häusler, R.E., Kleines, M., Uhrig, H., Hirsch, H.J. & Smets, H. Overexpression of phosphoenolpyruvate carboxylase from *Corynebacterium glutamicum* lowers the CO_2 compensation point (Γ*) and enhances dark and light respiration in transgenic potato. *J. Exp. Bot.* **50**, 1231–1242 (1999).
22. Whitney, S.M., Baldet, P., Hudson, G.S., Andrews, T.J. & Form, I. Rubiscos from non-green algae are expressed abundantly but not assembled in tobacco chloroplasts. *Plant J.* **26**, 535–547 (2001).
23. Zhu, X-G., Portis, A.R. & Long, S.P. Would transformation of C3 crop plants with foreign Rubisco increase productivity? A computational analysis extrapolating from kinetic properties to canopy photosynthesis. *Plant Cell Environ.* **27**, 155–165 (2004).
24. Edwards, G.E., Franceschi, V.R. & Voznesenskaya, E.V. Single cell C4 photosynthesis versus dual-cell (Kranz) paradigm. *Annu. Rev. Plant Biol.* **55**, 173–196 (2004).
25. Häusler, R.E., Hirsch, H.J., Kreuzaler, F. & Peterhansel, C. Overexpression of C_4-cycle enzymes in transgenic C_3 plants: a biotechnological approach to improve C_3-photosynthesis. *J. Exp. Bot.* **53**, 591–607 (2002).
26. Leegood, R.C. C_4 photosynthesis: principles of CO_2 concentration and prospects for its introduction into C_3 plants. *J. Exp. Bot.* **53**, 581–590 (2002).
27. Reumann, S. & Weber, A.P.M. Plant peroxisomes respire in the light: some gaps of the photorespiratory C2 cycle have become filled–others remain. *Biochim. Biophys. Acta–Mol. Cell Res.* **1763**, 1496–1510 (2006).
28. Long, S.P., Zhu, X-G., Naidu, S.L. & Ort, D.R. Can improvement in photosynthesis increase crop yields? *Plant Cell Environ.* **29**, 315–330 (2006).
29. Von Caemmerer, S. C4 photosynthesis in a single C3 cell is theoretically inefficient but may ameliorate internal CO_2 diffusion limitations of C3 leaves. *Plant Cell Environ.* **26**, 1191–1197 (2003).
30. Ku, S.B. & Edwards, G.E. Oxygen inhibition of photosynthesis. I. Temperature dependence and relation to O_2/CO_2 solubility ratio. *Plant Physiol.* **59**, 986–990 (1977).
31. Kruger, E.L. & Volin, J.C. Reexamining the empirical relation between plant growth and leaf photosynthesis. *Funct. Plant Biol.* **33**, 421–429 (2006).
32. Long, S.P., Ainsworth, E.A., Leakey, A.D., Nosberger, J. & Ort, D.R. Food for thought: lower-than-expected crop yield stimulation with rising CO2 concentrations. *Science* **312**, 1918–1921 (2006).
33. Paul, M.J. & Pellny, T.K. Carbon metabolite feedback regulation of leaf photosynthesis and development. *J. Exp. Bot.* **54**, 539–547 (2003).

34. Lefebvre, S., Lawson, T., Zakhleniuk, O.V., Lloyd, J.C. & Raines, C.A. Increased sedoheptulose-1,7-bisphosphatase activity in transgenic tobacco plants stimulates photosynthesis and growth from an early stage in development. *Plant Physiol.* **138**, 451–460 (2005).
35. Miyagawa, Y., Tamoi, M. & Shigeoka, S. Overexpression of a cyanobacterial fructose-1,6-sedoheptulose-1,7-bisphosphatase in tobacco enhances photosynthesis and growth. *Nat. Biotechnol.* **19**, 965–969 (2001).
36. Tolbert, N.E., Yamazaki, R.K. & Oeser, A. Localization and properties of hydroxypyruvate and glyoxylate reductases in spinach leaf particles. *J. Biol. Chem.* **245**, 5129–5136 (1970).
37. Kisaki, T. & Tolbert, N.E. Glycolate and glyoxylate metabolism by isolated peroxisomes or chloroplasts. *Plant Physiol.* **44**, 242–250 (1969).
38. Oliver, D.J. Role of glycine and glyoxylate decarboxylation in photorespiratory CO_2 release. *Plant Physiol.* **68**, 1031–1034 (1981).
39. Zelitch, I. The photooxidation of glyoxylate by envelope-free spinach chloroplasts and its relation to photorespiration. *Arch. Biochem. Biophys.* **150**, 698–707 (1972).
40. Igamberdiev, A.U. & Lea, P.J. The role of peroxisomes in the integration of metabolism and evolutionary diversity of photosynthetic organisms. *Phytochemistry* **60**, 651–674 (2002).
41. Herman, P.L., Ramberg, H., Baack, R.D., Markwell, J. & Osterman, J.C. Formate dehydrogenase in *Arabidopsis thaliana*: overexpression and subcellular localization in leaves. *Plant Sci.* **163**, 1137–1145 (2002).
42. Koncz, C. & Schell, J. The promoter of T_L-DNA gene *5* controls the tissue-spezific expression of chimaeric genes carried by a novel type of *Agrobacterium* binary vector. *Mol. Gen. Genet.* **204**, 383–396 (1986).
43. Reichel, C. *et al.* Enhanced green fluorescence by the expression of an Aequorea victoria green fluorescent protein mutant in mono- and dicotyledonous plant cells. *Proc. Natl. Acad. Sci. USA* **93**, 5888–5893 (1996).
44. Clough, S.J. & Bent, A.F. Floral dip: a simplified method for *Agrobacterium*-mediated transformation of *Arabidopsis thaliana*. *Plant J.* **16**, 735–743 (1998).
45. Goyal, A., Betsche, T. & Tolbert, N.E. Isolation of intact chloroplasts from *Dunaliella tertiolecta*. *Plant Physiol.* **88**, 543–546 (1988).
46. Gutheil, W.G. A sensitive equilibrium-based assay for D-lactate using D-lactate dehydrogenase: application to penicillin-binding protein/DD-carboxypeptidase activity assays. *Anal. Biochem.* **259**, 62–67 (1998).
47. Gotto, A.M. & Kornberg, H.L. The metabolism of C2 compounds in micro-organisms. 7. Preparation and properties of crystalline tartronic semialdehyde reductase. *Biochem. J.* **81**, 273–284 (1961).
48. Stitt, M., Lilley, R., Gerhardt, R. & Heldt, H. Determination of metabolite levels in specific cells and subcellular compartments of plant leaves. *Methods Enzymol.* **174**, 518–552 (1989).
49. Wagner, C., Sefkow, M. & Kopka, J. Construction and application of a mass spectral and retention time index database generated from plant GC/EI-TOF-MS metabolite profiles. *Phytochemistry* **62**, 887–900 (2003).